23rd ABCM International Congress of Mechanical Engineering
December 6-11, 2015, Rio de Janeiro, RJ, Brazil

INFLUENCE OF AXIAL LOADS ON THE STABILITIES AND NON-LINEAR DYNAMIC BEHAVIOUR OF THIN-WALLED OPEN SECTION ELEMENTS

Eulher C. Carvalho
Federal Institute of Education, Science and Technology of Goiás, IFG. Rua Maria Vieira Cunha, 775, Residencial Flamboyant, CEP 75804-714 – Jataí, GO, Brasil.
eulher.carvalho@ifg.edu.br

Paulo B. Gonçalves
Renzo C. Mancilla
Pontifical Catholic University of Rio de Janeiro, PUC-Rio. Rua Marquês de São Vicente, 225, Gávea, CEP 22451-900 – Rio de Janeiro, RJ, Brasil.
paulo@puc-rio.br, rcm1111@hotmail.com

Abstract. *The improvements of the manufacturing processes have led to lighter, stronger and slender structural elements, increasing the importance of researches in this field to ensure that their design is safe under different load conditions. Here, the non-linear dynamic vibrations of a simple supported one-dimensional thin-walled element with open section are investigated. Special attention is given to the influence of the axial load on the bifurcations and instabilities of the element. For this, a model based on the modified Vlasov's theory is adopted, were warping, shortening and flexural-torsional coupling effects are taken into account, as well as, inertial and geometric non-linarites. By using several tools of non-linear dynamics, a complex dynamic behavior is observed, principally in the 1:1 external resonance region. The results show that the axial load changes the non-linear behavior of the element. In addition, bifurcations leading to multiple coexisting solutions are observed.*

Keywords: *nonlinear vibrations, thin-walled section, open section, axial load.*

1. INTRODUCTION

Due to their structural efficiency, thin-walled elements with open sections are commonly used in several engineering applications, mainly working under bending or compressive axial loads. Thin-walled elements with open cross-section usually have low torsional stiffness (Murray, 1986, Mori and Munaiar, 2009 and Allen and Bulson, 1980). Such slender elements can display several types of instability in the presence of axial excitations. Many of the usual cross sections, such as the channel section, have only one symmetry axes (mono-symmetric section) and the probability of flexural-torsional coupled motions increases. In this context, it is essential to know accurately the nonlinear dynamic behavior of highly flexible elements with thin-walled open cross sections and the possible instability phenomena and obtain the associated instability boundaries in the force control space.

Nevertheless, and despite the extensive literature on metallic elements with open cross section, usually based on the formulations proposed by Timoshenko and Young (1955), Gere and Lin (1958) and Vlasov (1961), little is known about their non-linear dynamic behavior and instabilities. Structural analyses based on Vlasov's theory include those by Black (1967), Barsoum and Gallagher (1970), Gobarah and Tso (1971), Wang and Kitipornchai (1986), Moore (1986), Laudiero and Zaccaria (1988) and Trahair (1993), among others.

Originally, Vlasov's formulation neglected some terms related to the geometric non-linearity imposed by large lateral displacements and torsion angles. These terms were included by Attard (1986), Ronagh *et al*. (2000) and Mohri *et al*. (2001). Subsequently the last formulation was used in several papers to study the linear vibration and buckling of several metallic profiles (Mohri et al., 2003, 2004, 2008, 2010 and 2013). Mancilla et al. (2014), using this formulation, studied the nonlinear dynamics of a channel section under lateral loads. In addition, Schulz and Filippou (1998) developed a model for non-uniform warping and Di Egidio, Luongo and Vestroni (2003a, 2003b) derived a non-linear mechanical model, were the warping was obtained extending the Vlasov's theory into the non-linear regime.

In this work, the nonlinear vibrations and possible dynamic instabilities in a simply-supported one-dimensional thin-walled element with an open channel section under axial load is studied using a non-linear model based on the modified Vlasov's theory (Mohri *et al*., 2001). The effects of large displacements and torsion angles, warping, axial shortening and flexural-torsional coupling are taken into account. Special attention is given to the influence of a harmonic axial load on the dynamic behavior of the element. Several tools of nonlinear dynamics, such as time responses, phase-space portraits, Poincaré maps, bifurcation diagrams and basins of attraction are used to unveil the dynamics of the column.

2. DYNAMIC SYSTEM

A simply-supported column element with mono-symmetric channel section with length L and mass per unit length m is considered. Figure 1 shows an undeformed segment of the element together with the adopted rectangular coordinate system (X, Y and Z), geometric properties of the cross section and loads. Here CG is the center of gravity and SC is the shear center. The shear center coordinates are given by y_{sc} and z_{sc}. In addition, b is the profile width, h, its height, t_w, the web thickness, t_f, the flange thickness and M is a point on the section contour with its coordinates (y, z; ζ), where ζ is the sectorial coordinate of a point as defined in Vlasov's model for non-uniform torsion (Mohri et al. 2004). An linear, elastic, isotropic material with Young's modulus E and Poisson's ratio ν is considered.

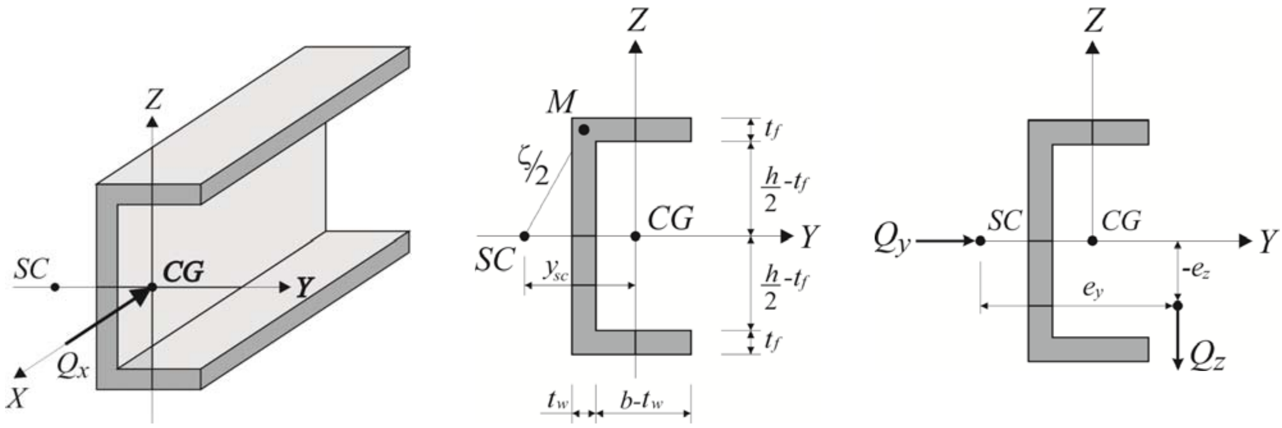

a) Coordinate system and axial load   b) Cross section dimensions   c) Lateral loads

Figure 1. Mono-symmetric channel section.

The element can be subjected to an axial load given by $Q_x = p_x + q_x \cos(\Omega_x t)$, where p_x is the static load and $q_x \cos(\Omega_x t)$ is a harmonic excitation with frequency Ω_x, magnitude q_x (t is the time). In the Y direction a uniformly distributed lateral harmonic excitation defined by $Q_y = 1.10^{-3}\cos(\Omega_y t)$ (small perturbation) is considered. $Q_z = 0.00$ in this analysis.

3. EQUATIONS OF MOTION

After consider only the first vibration mode in the Galerkin approximation method, the following three coupled nonlinear equations of motion are obtained:

$$\frac{m L^2}{\pi^2}\left(\ddot{v}_0 + z_{sc}\,\ddot{\theta}_0\right) + \left(2\,\xi\,\omega_0\right)\dot{v}_0 + P_z\left(v_0 + \frac{\pi^2}{8L^2}v_0^3\right) - Q_x\left(v_0 + z_{sc}\,\theta_0\right) - \frac{4P}{3\pi}y_{sc}\,\theta_0^2 + \left(P_z - P_y\right)\left(\frac{8}{3\pi}w_0\,\theta_0 - \frac{3}{4}v_0\,\theta_0^2\right) - \frac{32}{\pi^3}M_{0y} = 0 \tag{1}$$

$$\frac{m L^2}{\pi^2}\left(\ddot{w}_0 - y_{sc}\,\ddot{\theta}_0\right) + \left(2\,\xi\,\omega_0\right)\dot{w}_0 + P_y\left(w_0 + \frac{\pi^2}{8L^2}w_0^3\right) - Q_x\left(w_0 - y_{sc}\,\theta_0\right) - \frac{4P}{3\pi}z_{sc}\,\theta_0^2 + \left(P_z - P_y\right)\left(\frac{8}{3\pi}v_0\,\theta_0 + \frac{3}{4}w_0\,\theta_0^2\right) - \frac{32}{\pi^3}M_{0z} = 0 \tag{2}$$

$$\frac{m L^2}{\pi^2}\left(I_0\,\ddot{\theta}_0 + z_{sc}\,\ddot{v}_0 - y_{sc}\,\ddot{w}_0\right) + \left(2\,\xi\,\omega_0\right)\dot{\theta}_0 + I_0\,P_\theta\,\theta_0 + \frac{3\pi^2 E I_t}{8L^2}\theta_0^3 - Q_x\left(I_0\,\theta_0 + z_{sc}\,v_0 - y_{sc}\,w_0\right) + \left(P_z - P_y\right)\left(\frac{8}{3\pi}v_0\,w_0 - \frac{3}{4}\theta_0\,v_0^2 + \frac{3}{4}\theta_0\,w_0^2\right) + Q_x\left(\frac{8\,z_{sc}}{3\pi}w_0\,\theta_0 - \frac{8\,y_{sc}}{3\pi}v_0\,\theta_0\right) - M_{0z}\left(\frac{32}{\pi^3}e_y - \frac{8}{\pi^2}e_z\,\theta_0\right) = 0 \tag{3}$$

where v_0 and w_0 are the deflections of the element in Y and Z directions, respectively, θ_0 is the torsion angle, ξ is the damping ratio, ω_0 is the lowest natural frequency, I_0 is the polar moment of inertia about shear center, I_t is a higher order geometric constant, P_y and P_z are the classical Eulher buckling loads in Y and Z directions, respectively, P_θ is the buckling torsion load, Q_x is the compressive axial load and, finally, M_{0y} and M_{0z} are the bending moments about Y and Z axes due to the lateral load Q_y, being:

$$I_t = I_R - A I_0^2 \tag{4}$$

$$P_y = \frac{\pi^2 E I_y}{L^2} \tag{5}$$

$$P_z = \frac{\pi^2 E I_z}{L^2} \tag{6}$$

$$P_\theta = \frac{1}{I_0}\left(\frac{\pi^2 E I_\zeta}{L^2} + \frac{E J}{2(1+\nu)}\right) \tag{7}$$

$$M_{0y} = \frac{Q_y L^2}{8} \tag{8}$$

$$M_{0z} = \frac{Q_z L^2}{8} = 0 \tag{9}$$

Here, I_R is the fourth moment of inertia about shear center, I_y and I_z are the principal moment of inertia about Y and Z axes, respectively, I_ζ is the warping constant, J is the St-Venant torsion constant, E is the elastic modulus, A is the cross-section area and ν is the Poisson's ratio, where:

$$I_R = {}_A\!\int (y - y_{sc})^4 \, dA + {}_A\!\int 2\,(y - y_{sc})\,(z - z_{sc})\, dA + {}_A\!\int (z - z_{sc})^4 \, dA \tag{10}$$

$$I_y = {}_A\!\int z^2 \, dA \tag{11}$$

$$I_z = {}_A\!\int y^2 \, dA \tag{12}$$

$$I_\zeta = {}_A\!\int \zeta^2 \, dA \tag{13}$$

$$J \cong \frac{1}{3}\left(b t_f^3 + h t_w^3 + b t_f^3\right) \tag{14}$$

Details of this formulation can be found in Mohri *et al*. (2001).

4. NUMERICAL RESULTS

For the numerical analysis, a steel column with elastic modulus E = 210.00 GPa, Poisson's ratio ν = 0.30 and mass density ρ = 7800.00 kgf/m³ is adopted. The following geometric parameters are considered: length L = 400.00 cm, width b = 10.00 cm, height h = 20.00 cm, web thickness t_w = 0.50 cm, flange thickness t_f = 0.50 cm, shear centre coordinates y_{sc} = 6.0818 cm and z_{sc} = 0.00 cm and cross-section area A = 19.50 cm², warping constant I_ζ = 12888.00 cm^4, principal moments of inertia I_y = 1236.60 cm^4 and I_z = 193.45 cm^4, fourth moment of inertia I_R = 350530.00 cm^6 and St-Venant torsion constant J = 1.67 cm^4.

The usual linear variation of the lowest natural frequency squared as a function of the compressive static axial load p_x is shown in Fig.2a. As the axial load increases the frequency decreases, becoming zero when the axial load reaches the critical value. The lowest natural frequency of the simply-supported unloaded element is ω_0 = 100.81 rad.s^{-1}, while its critical load is P_{cr} = 250.50 kN.

The axial load also has a significant influence on the nonlinear frequency-amplitude relation associated with the lowest natural frequency, as shown in Fig. 2b. The unloaded element exhibits a small degree of nonlinearity of the hardening type (curve A), which increases as the load increases (B and C curves).

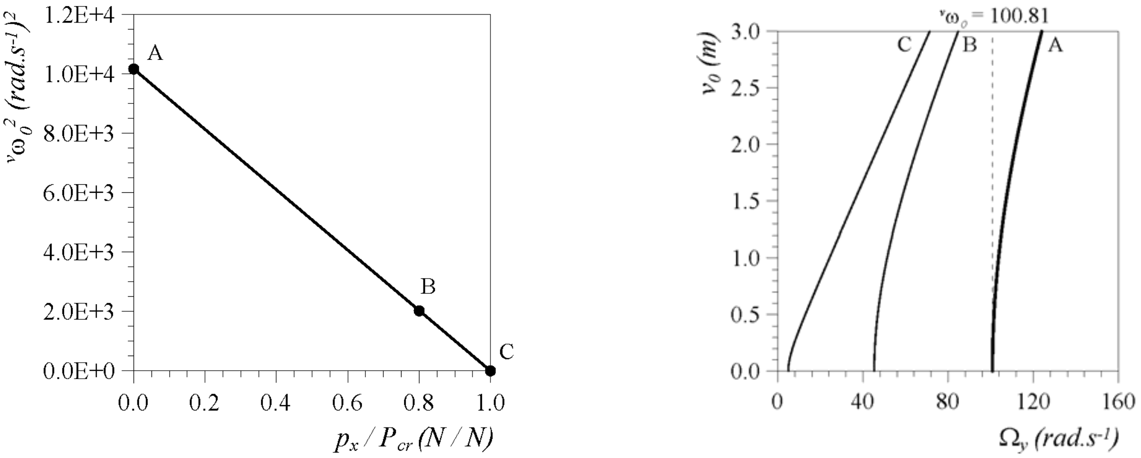

a) Axial load-frequency relation

b) Frequency-amplitude relations

Figure 2. Influence of axial static load on the lowest natural frequency and on the nonlinear frequency-amplitude relation.

At this point, the parametric instability of the structural element subject to a harmonic axial load, $q_x \cos(\Omega_x t)$, is studied is investigated assuming a damping ratio of $\xi = 0.3\%$. Fig. 3 shows the parametric instability boundary of the element in the excitation frequency (Ω_x) - excitation magnitude (q_x) control space. It is the threshold beyond which infinitesimal perturbations of the trivial solution result in an initial exponential growth of the oscillations, leading to an oscillatory non-trivial response. The parametric instability boundary is composed by various curves, each one associated with a particular local bifurcation event. The first important instability region is associated with the fundamental resonance zone when the frequency of excitation is equal to the lowest natural frequency of the element ($\Omega_x = {}^{v}\omega_0$ = 100.81 rad.s^{-1}). The second V-shaped region to the right is associated with the principal parametric instability region and occurs when the frequency of excitation is equal to two times the lowest natural frequency of the element ($\Omega_x = 2\ {}^{v}\omega_0$ = 201.62 rad.s^{-1}). The smaller V-shape regions to the left are related to super-harmonic resonances. Usually the column is subjected to a static preload p_x in addition to the harmonic axial excitation. As the static preload increases the natural frequency decreases, the parametric instability boundary moves to the left as illustrated in Fig. 4 for p_x =200kN.

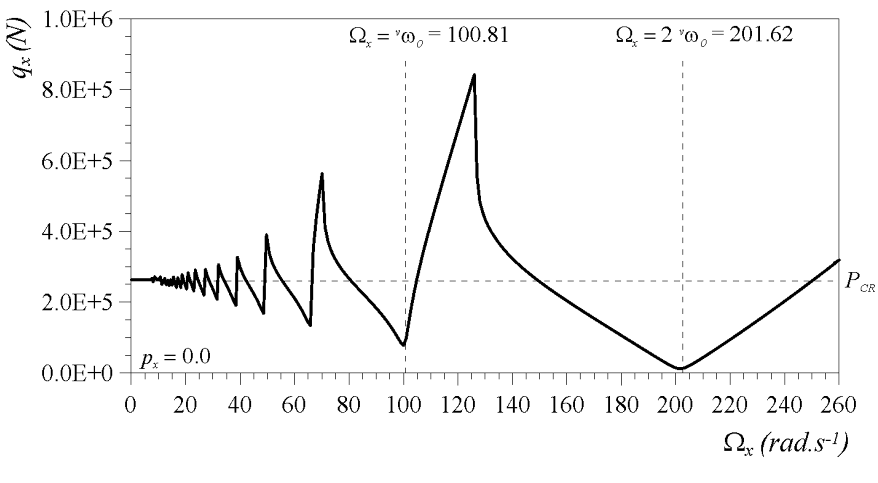

Figure 3. Parametric instability boundary in the force control space. Axial load: $q_x \cos(\Omega_x t)$.

To understand the loss of stability of the column and the bifurcations associated with the instability boundary, a study of the three-dimensional motions of the element in the two main parametric instability regions is carried out. As a starting point, Fig. 5 displays the bifurcation diagram for $\Omega_x = 2\ {}^{v}\omega_0$. This bifurcation diagram is obtained using the brute force algorithm and taking the magnitude of the axial excitation q_x as the control parameter.

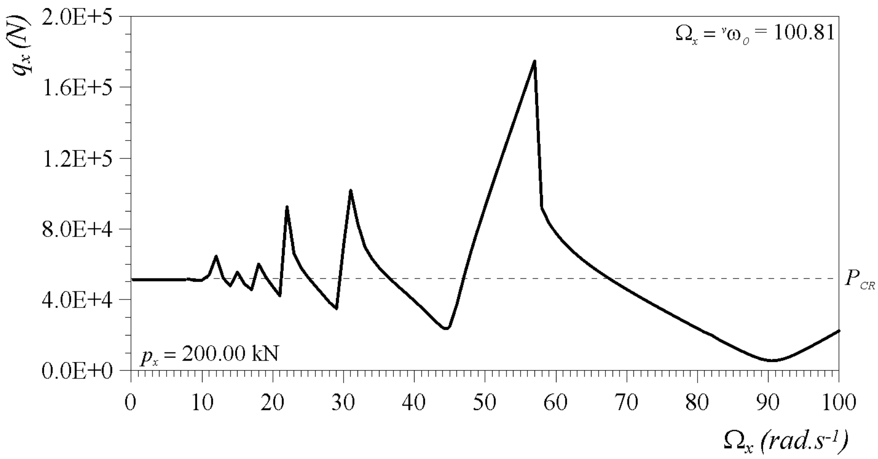

Figure 4. Parametric instability boundary in the force control space. Axial load: $200.10^3 + q_x \cos(\Omega_x t)$.

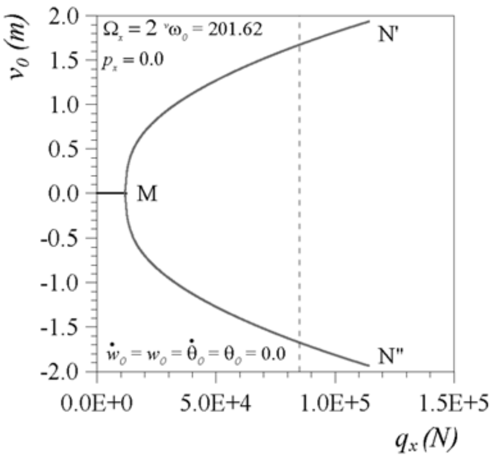

Figure 5. Bifurcation diagram of the Poincaré map for the column subject to an axial load with $\Omega_x = 2\ {}^v\omega_0$.

In Fig. 5 two classes of solution are identified: the trivial solution identified as M solution (black branch) and a period two non-trivial solution identified as N (',"). As the load increases, the trivial solution becomes unstable due to a supercritical pitchfork bifurcation, and the response changes to a stable periodic solution with a period equal to two times the excitation period. A time and phase-space responses of these solutions are illustrated in Fig. 6, considering $q_x = 85.00$ kN. The angle of torsion for these solutions is zero, the motion occurs in the Y direction (direction with lowest moment of inertia). In addition, Fig. 7 shows a cross section of the six-dimensional basin of attraction. In this cross-section (where all remains phase-space variables are zero) only one region is observed, as expected, which is associated with the non-trivial solution.

Figure 8 shows the bifurcation diagram for $\Omega_x = {}^v\omega_0$, which corresponds to the lowest critical load in the secondary (i.e., fundamental) region of parametric instability (see Figure 3). The trivial solution (S) becomes unstable at $q_x \approx 89.95$ kN. The structure goes through a subcritical bifurcation, leading to two (out-of-phase) uncoupled period one responses (R and T), as shown in Fig. 9 for $q_x = 85.00$ kN. Thus, between $q_x \approx 79.05$ kN and $q_x \approx 85.95$ kN, three coexisting periodic solutions are observed and the behavior of the element has an initial conditions dependence.

Figure 10 shows selected cross sections of the six-dimensional basin of attraction for $q_x = 85.00$ kN. Most of the initial conditions converge to the trivial solution (fixed point S associated with black basin). Sets of initial conditions converge to nontrivial solutions R (dark gray basin) or S (light gray basin) when v_0 is different to zero. A high sensitivity is observed in Fig. 10c and Fig. 10d, were many initial conditions (white basin) can provoke a structural collapse (exponential growth of the oscillations). Coupled flexural-torsional solutions are not detected.

5. CONCLUSIONS

A nonlinear formulation including the geometric nonlinearities is adopted to investigate the response of a simply-supported steel column subjected to static plus harmonic axial load. Bifurcation diagrams, phase-space portraits, time responses, Poincaré maps and basins of attraction are used to explore the behavior of the beam in the principal (1:2 external resonance) and fundamental (1:1 external resonance) resonance regions.

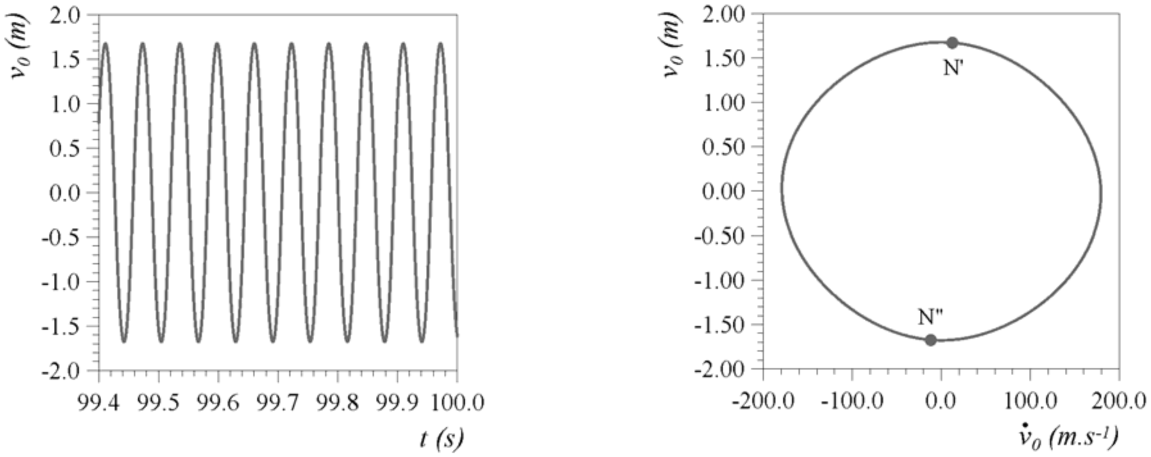

a) Time response

b) Phase-space response and Poincare section

Figure 6. Stable coexisting solutions at q_x = 85.00 kN and $\Omega_x = 2\,^v\omega_0$.

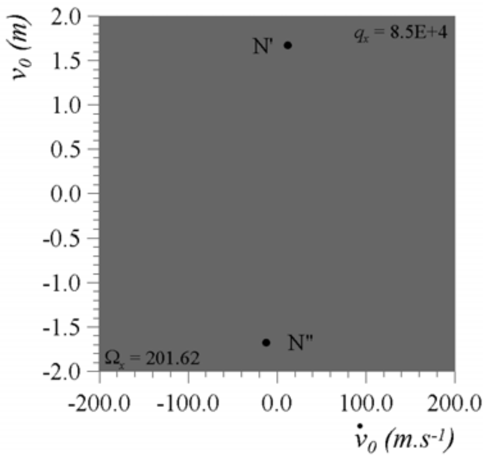

Figure 7. Cross-section of the basin of attraction at q_x = 85.00 kN and $\Omega_x = 2\,^v\omega_0$.

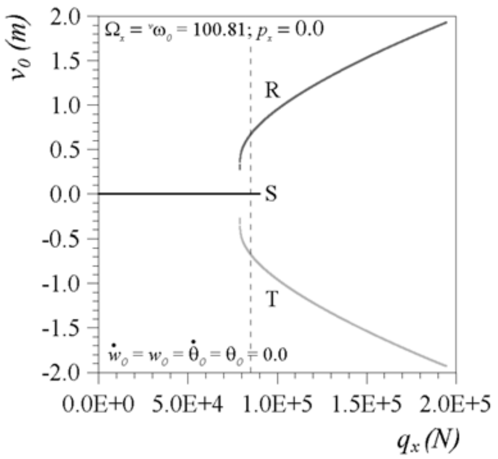

Figure 8. Bifurcation diagram of the Poincare map for the element subject to an axial load at $\Omega_x = {}^v\omega_0$.

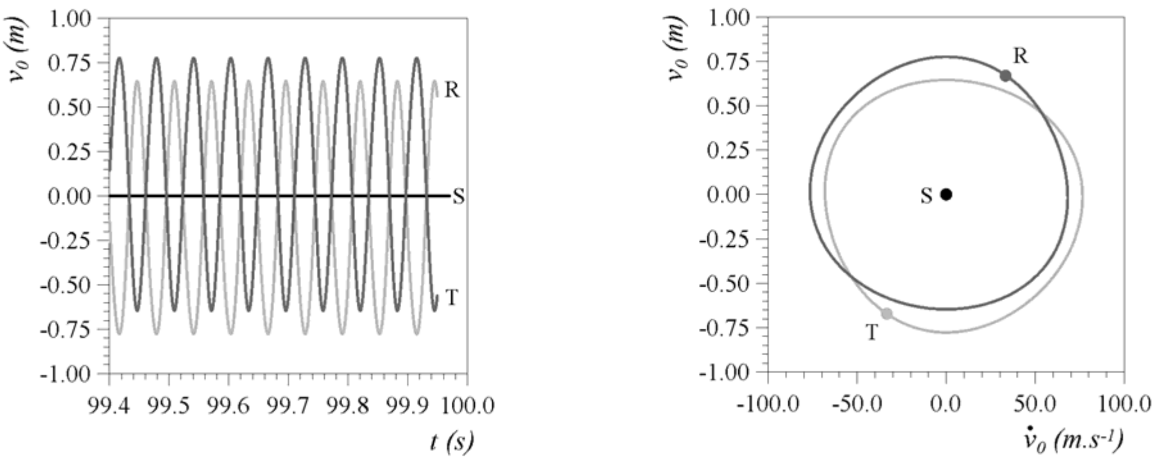

a) Time response

b) Phase-space response and Poincare section

Figure 9. Stable coexisting solutions at q_x = 85.00 kN and $\Omega_x = {}^v\omega_0$.

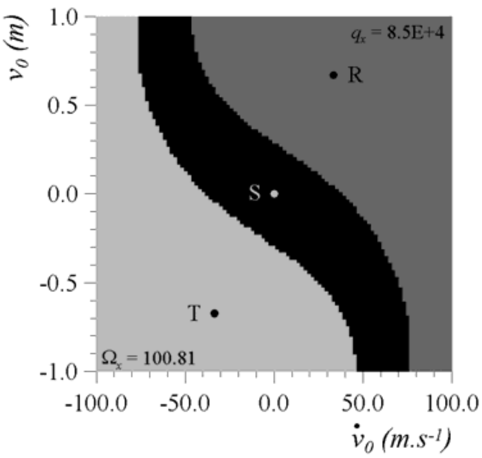

a) Cross-section v_0 vs. $\dot{v}_0$.

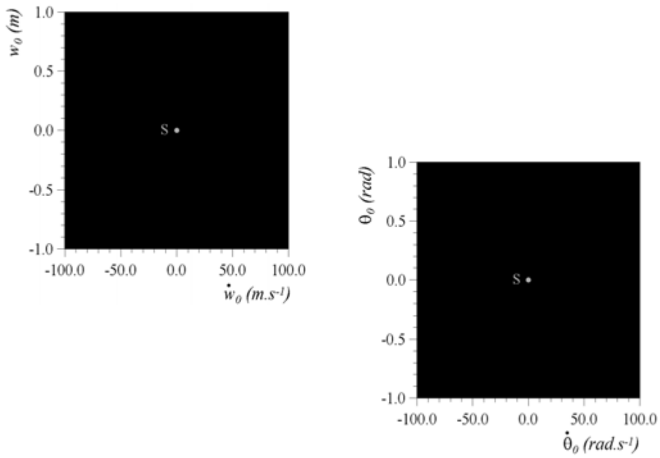

b) Cross-section w_0 vs. $\dot{w}_0$ and θ_0 vs. $\dot{\theta}_0$.

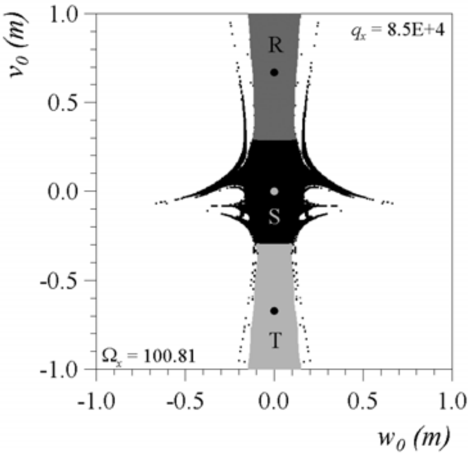

c) Cross-section v_0 vs. w_0.

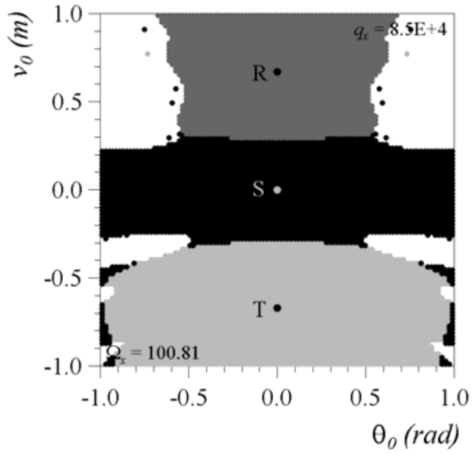

d) Cross-section v_0 vs. θ_0.

Figure 10. Cross-sections of the basin of attraction at q_x = 85.00 kN and $\Omega_x = {}^{v}\omega_0$.

Due to the cross-section geometry and loading conditions, the beam exhibits only planar displacements in the direction of the lowest moment of inertia. The static axial load has a profound influence on the frequency-amplitude relation and on the resonance curves of the element. The bifurcation analysis shows that the element under harmonic axial excitation displays a complex non-linear dynamic behavior. Finally, the paper shows how the tools of nonlinear dynamics can help in the understanding of the global safety and integrity of the model, thus leading to a safe structural design.

6. ACKNOWLEDGEMENTS

The authors gratefully acknowledge the support of CAPES, CNPq, PUC-Rio and NEPE - IFG.

7. REFERENCES

Allen H.G. and Bulson P.S., *Background to buckling*, London: McGraw-Hill, 1980.

Attard, M.M., "Nonlinear theory of non-uniform torsion of thin-walled open beams", *Thin-walled Structures*, vol. 4, pp. 101-134, 1986.

Barsoum, R.S. and Gallagher, R.H. "Finite element analysis of torsional and torsional-flexural stability problems", *International Journal for Numerical Methods in Engineering*, vol. 2, pp. 335-352, , 1970.

Black, M.M., *Non-linear behaviour of thin-walled unsymmetric beam sections subject to bending and torsion.* Thin-walled structures, London: Chatto and Windus, 1967.

Di Egidio, A., Luongo, A. and Vestroni, F., "A nonlinear model for open cross section thin-walled beams – Part I: Formulation", *Int. J. Non-Linear Mech.*, vol. 38, n. 7, pp. 1067-1081, 2003a.

Di Egidio, A., Luongo, A. and Vestroni, F., "A nonlinear model for open cross section thin-walled beams – Part II: Forced motion", *Int. J. Non-Linear Mech.*, vol. 38, n. 7, pp. 1083-1094, 2003b.

Gere, J.M. and Lin, Y.K., "Coupled vibrations of thin-walled beams of open-cross section", *Journal of Applied Mechanics*, vol. 80, pp. 373-378, 1958.

Gobarah, A.A. and Tso, W.K., "A non-linear thin-walled beam theory", *International Journal of Mechanical Science*, vol. 13, pp. 1025-1038, 1971.

Gonçalves, P. B., Silva, F. M. A., Rega, G., Lenci, S., Global dynamics and integrity of a two-d.o.f. model of a parametrically excited cylindrical shell, *Nonlinear Dynamics*, vol. 63, pp. 61-82, 2011

Laudiero, F. and Zaccaria, D., "Finite element analysis of stability of thin-walled beams of open section", *International Journal of Mechanical Science*, vol. 30, n. 8, pp. 543-557, 1988.

Mancilla, R.C., Gonçalves, P.B., Carvalho, E.C., "Vibrações não lineares de perfis esbeltos com seção aberta". In: *XXXV Ibero-Latin American Congress on Computational Methods in Engineering - CILAMCE 2014*, 2014, Fortaleza - CE - Brasil. Proceedings of CILAMCE 2014, 2014.

Mohri, F., Azrar, L. and Potier-Ferry, M., "Flexural–torsional post-buckling analysis of thin-walled elements with open sections", *Thin-walled structures*, vol. 39, n. 11, p. 907-938, 2001.

Mohri, F., Azrar, L. and Potier-Ferry, M., "Vibration Analysis of buckled thin-walled beams with open sections", *Journal of Sound and Vibration*, vol. 275, pp. 434-446, 2004.

Mohri, F., Bouzerira, C. and Potier-Ferry, M., "Lateral buckling of thin-walled beam-column elements under combined axial and bending loads", *Thin-Walled Structures*, vol. 46, n. 3, pp. 290-302, 2008.

Mohri, F., Brouki, A. and Roth, J.C., "Theoretical and numerical stability analyses of unrestrained, mono-symmetric thin-walled beams", *Journal of Constructional Steel Research*, vol. 59, n. 1, pp. 63-90, 2003.

Mohri, F., Damil, N. and Potier-Ferry, M., "Buckling and lateral buckling interaction in thin-walled beam-column elements with mono-symmetric cross sections", *Applied Mathematical Modelling*, n. 37, pp. 3526-3540, 2013.

Mohri, F., Damil, N. and Potier-Ferry, M., "Large torsion finite element model for thin-walled beams", *Computers and Structures*, n. 86, pp. 671-683, 2008.

Mohri, F., Damil, N. and Potier-Ferry, M., "Linear and non-linear stability analyses of thin-walled beams with monosymmetric I sections", *Thin-Walled Structures*, vol. 48, n. 4, pp. 299-315, 2010.

Moore, D.B., "A non-linear theory for the behaviour of thin-walled sections subjected to combined bending and torsion", *Thin-walled Structures*, vol. 4, pp. 449-466, 1986.

Mori, D.D. and Munaiar, N.J., *Flexo torção: barras de seção delgada aberta*, EESC-USP, 2009.

Murray, N.W., *Introduction to the theory of thin-walled structures*, Oxford: Clarendon Press, 1986.

Ronagh, H.R., Bradford, M.A. and Attard, M.M., "Nonlinear analysis of thin-walled members of variable cross-section. Part I: Theory", *Computers and Structures*, vol. 77, pp. 285-299, 2000.

Schulz, M. and Filippou, C., "Generalized warping torsion formulation", *Journal of Engineering Mechanics*, vol. 124, pp. 339-347, 1998.

Timoshenko, S. and Young, D.H., *Vibration problems in engineering*, New Jersey: Van Nostrand, 1955.

Trahair, N.S., *Flexural–torsional buckling of structures*, London: Chapman and Hall, 1993.

Vlasov, V.Z., *Thin-walled elastic beams*, Israel Prog. for Scientific Translations, Jerusalem, 1961.

Wang, C.M. and Kitipornchai, S., "On stability of monosymmetric cantilevers", *Engineering Structures*, vol. 8, pp. 169-180, 1986.

8. RESPONSIBILITY NOTICE